Curvature-Guided Motility of Microalgae in Geometric Confinement

Tanya Ostapenko,[1] Fabian Jan Schwarzendahl,[1,2] Thomas J. Böddeker,[1] Christian Titus Kreis,[1,2] Jan Cammann,[1] Marco G. Mazza,[1] and Oliver Bäumchen[1*]

[1]*Max Planck Institute for Dynamics and Self-Organization (MPIDS), Am Faßberg 17, D-37077 Göttingen, Germany*

[2]*Georg-August-Universität Göttingen, Friedrich-Hund-Platz 1, D-37077 Göttingen, Germany*

(Received 8 May 2017; published 7 February 2018)

Microorganisms, such as bacteria and microalgae, often live in habitats consisting of a liquid phase and a plethora of interfaces. The precise ways in which these motile microbes behave in their confined environment remain unclear. Using experiments and Brownian dynamics simulations, we study the motility of a single *Chlamydomonas* microalga in an isolated microhabitat with controlled geometric properties. We demonstrate how the geometry of the habitat controls the cell's navigation in confinement. The probability of finding the cell swimming near the boundary increases with the wall curvature, as seen for both circular and elliptical chambers. The theory, utilizing an asymmetric dumbbell model of the cell and steric wall interactions, captures this curvature-guided navigation quantitatively with no free parameters.

DOI: 10.1103/PhysRevLett.120.068002

Life in complex geometries can manifest itself at the microscopic level through the myriad of ways in which microorganisms interact with their environment. This entails a broad spectrum of microbiological phenomena, ranging from amoebic crawling [1,2] and fibroblast migration [3], the directional migration of epithelial cells on curved surfaces [4], and microbial proliferation in space-limited environments [5] to the motility of biological microswimmers in confinement [6,7]. In fact, the natural habitats for microbial life are often nonbulk situations, including aqueous microdroplets [8] and the interstitial space of porous media, such as rocks [9,10] and soil [11]. The study of how self-propelled microorganisms in a liquid medium interact with their confining boundaries finds application in physiology with regards to spermatozoa motility in the reproductive tract [12–15], the motion of parasites in the vertebrate bloodstream [16], and in microbiology in the context of biofilm formation [17–20].

Upon interaction with a boundary, these microswimmers might undergo long-range hydrodynamic interactions, in addition to contact interactions [21,22]. For the description of their motility near interfaces, a distinction between "puller"- and "pusher"-type swimmers is required [23], since the flow fields around the two classes entail fundamental differences [24–28]. At flat interfaces, the contact of a spermatozoon's flagellum with a surface tends to rotate it towards a boundary, thus preventing these pusher-type swimmers from escaping flat or weakly-curved surfaces [29]. However, for the puller-type microswimmer, *Chlamydomonas*, a soil-dwelling microalga with two anterior flagella, steric interactions were found responsible for its microscopic scattering off of a flat interface [29]. Single scattering events of *Chlamydomonas* cells were also reported at convex interfaces, where two regimes emerge as the cell scatters off: an initial, contact force regime and a second, hydrodynamics-dominated regime [30]. Beyond these details of the microscopic interactions at interfaces, the way in which the motility of a single cell is affected by the geometry of a confining domain remains elusive.

In this Letter, we report on the motility of a single *Chlamydomonas* cell in tailor-made microhabitats to elucidate the effects of geometric confinement. We find that the dominant attributes of the swimming statistics are the alga's spatial confinement, which limits its motion to its swimming plane, and the compartment's curved boundary in this plane. Our experiments are in quantitative agreement with Brownian dynamics simulations, whose main ingredients are steric wall interactions and the alga's torque at the compartment interface during a finite interaction time. While a conclusive description of the microscopic details of wall interactions might remain debated today, our results illuminate how a single puller-type cell's navigation in confinement is primarily dominated by the details of the environment's geometric constraints.

We employed optical microscopy techniques and particle tracking to study the motility of a single wild-type *Chlamydomonas reinhardtii* cell (SAG 11-32b) contained within an isolated quasi-two-dimensional microfluidic compartment (see the Supplemental Material [31], Sec. S1 for details). We study precisely a single isolated cell in order to exclude any cell-cell interactions or collective effects. Experiments were performed in circular compartments with radii $r_c = 25$–500 μm, and elliptical chambers with comparable semiaxes dimensions. The height of all compartments was approximately 20 μm, about one cell diameter (body and flagella); thus, out-of-plane reorientations of the cell are inhibited. Each single-cell experiment was repeated up to 10 times using different

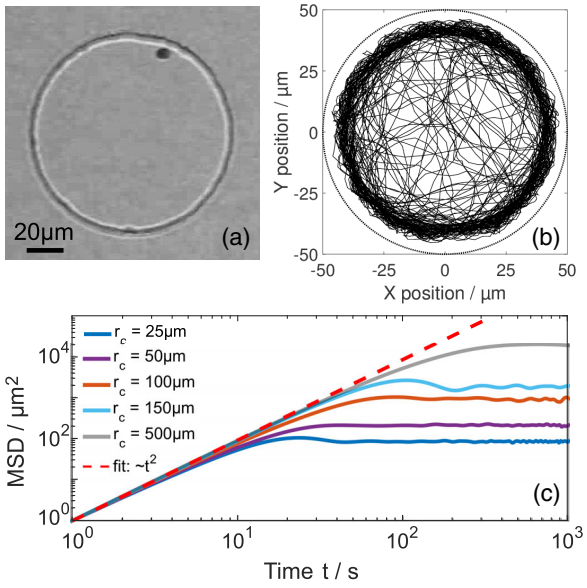

FIG. 1. Experimental design and trajectory analysis. (a) Optical micrograph of a single alga contained in a quasi-two-dimensional (2D) circular compartment. (b) Exemplar single-cell trajectory for $r_c = 50$ μm. (c) Mean-squared displacements (solid lines) for different compartment radii. The dashed line is a best fit to the short-time ballistic behavior ($\sim t^2$).

cells each time. Figure 1(a) displays an image from an experiment (Movie 1 in Ref. [31]) for $r_c = 50$ μm from which the trajectory of the alga's body center was extracted [Fig. 1(b)]. The alga's trajectory shows a higher density of trajectory points closer to the concave interface, as compared to the compartment's center, which we study in greater detail in this work.

We use the mean-squared displacement (MSD) to characterize the alga's swimming behavior. Here, the MSD for the observation time t was extracted from a single alga's experimental trajectory for each compartment size; see Fig. 1(c). We find that the MSD curves show no clear transition between ballistic behavior, i.e., MSD $\sim t^2$ on short time scales to diffusive, i.e., MSD $\sim t$ on long time scales, as reported in previous studies on *Chlamydomonas* swimming in unconfined 2D environments (transition time from ballistic to diffusive ~2 s) [29]. A linear fit to the initial regime of the experimental data yields an exponent of 1.90 ± 0.03, in approximate agreement with a regime of ballistic swimming. On long time scales, the MSD reaches a plateau corresponding to the explorable area of its confined environment. Hence, we find that the alga's run-and-tumble-like motion in environments unconfined in the swimming plane [35] becomes predominantly ballistic swimming in confinement.

The experimental cell trajectories were statistically averaged and converted into relative probability density maps. Figure 2 displays a series of 2D heat maps of the relative probability density of the cell's positions for different compartment sizes. Our experimental data provide evidence for a pronounced near-wall swimming effect inside the compartment, whose significance decreases for increasing compartment size. This near-wall swimming effect is further quantified by azimuthally collapsing the heat maps into radial probability densities, $P(r)$, as depicted in Fig. 3(a). We define $P(r)$ as:

$$P(r) = \frac{h(r)/(2\pi r \Delta r)}{\int_0^{r_c} \frac{h(r)}{2\pi r \Delta r} dr}, \tag{1}$$

where r is the distance from the center of the compartment, and $h(r)$ is the count of all the alga's positions in a circular shell at distance r with thickness Δr. In order to compare data from different compartment sizes, we normalize $P(r)$ such that $\int_0^{r_c} P(r) dr = 1$. Note that a homogeneous distribution of trajectory points would result in $P(r) = 1/r_c = \text{const}$ by this definition. We observe that $P(r)$ starts from a plateau in proximity of the compartment's center and increases significantly close to the wall. The lateral extent (full-width-half-maximum) of the peak of $P(r)$ ranges from 3–5 μm, about half a cell body diameter; the peak position is consistently 9–11 μm away from the wall. At the compartment wall, $P(r)$ drops off, representing a possible zone of flagella-wall contact interactions. As shown in Fig. 3(a), the maximum of $P(r)$ decreases for increasing compartment size, while the overall shape of $P(r)$ described above is preserved.

We compared these experimental results to Brownian dynamics simulations, where the *Chlamydomonas* cell is

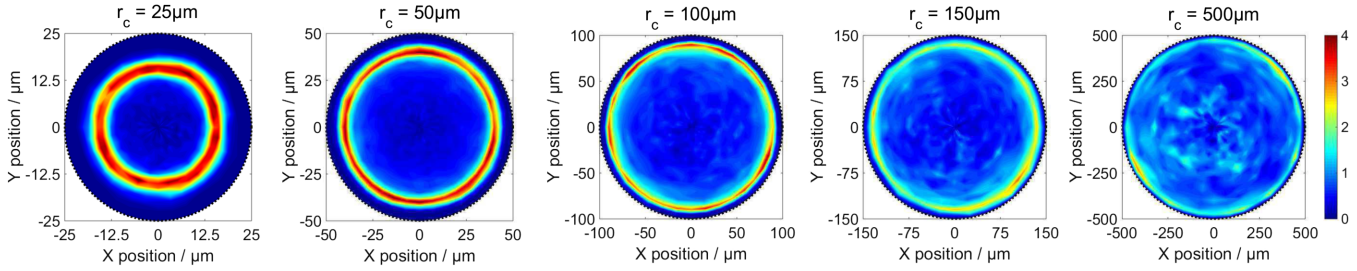

FIG. 2. Relative probability density for a single cell in circular confinement. Heat maps represent the alga's position obtained from experimental data for different compartment sizes: (L–R) $r_c = 25$ μm, 50 μm, 100 μm, 150 μm, 500 μm. Each map contains statistically averaged data from a minimum of 2–5 independent experiments.

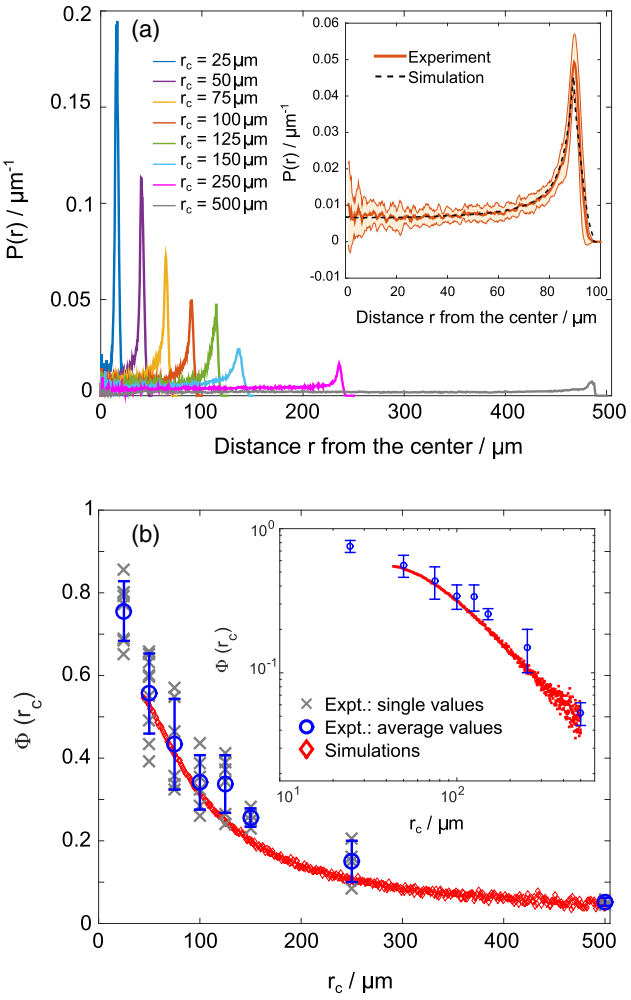

FIG. 3. (a) Radial probability densities $P(r)$ for compartment sizes, r_c, each from 2–10 independent experiments. (Inset) Close-up of the experimental data (average: solid line, standard deviation: background) and Brownian dynamics simulations (dashed line) for $r_c = 100$ μm. (b) Near-wall swimming probability $\Phi(r_c)$: experimental data (circles) denote mean values averaged over independent experiments (crosses) and Brownian dynamics simulations (diamonds). (Inset) Log-log representation of the same data.

modeled as an active asymmetric dumbbell (Sec. S2, Ref. [31]) consisting of two rigid spheres [36]. The smaller sphere represents the cell's body, and the larger sphere mimics the stroke-averaged area covered by the beating of the two anterior flagella. The Langevin equation represents a balance of forces, both deterministic and stochastic ones, experienced by the microswimmer [23]. The position $\vec{r}$ of the dumbbell's center of mass is described by the equation of motion

$$\frac{d\vec{r}}{dt} = v_0\vec{e} + \mu_w\vec{F}_w + \vec{\eta}. \tag{2}$$

Here, v_0 is the propulsion speed, $k_BT\mu_w$ denotes the diffusivity, μ_w is the mobility (ratio of velocity to an applied force), $\vec{F}_w$ is the force associated with the steric wall interaction (Weeks-Chandler-Andersen potential [37]) and $\vec{\eta}$ is a Gaussian white noise. The unit vector $\vec{e}$ represents the direction of the propulsion velocity pointing from the small to the large sphere. The orientational equation of motion is

$$\frac{d\vec{e}}{dt} = (\vec{T}_w/\tau_w + \vec{\xi}) \times \vec{e}, \tag{3}$$

where $\vec{T}_w$ is the torque acting at the wall, τ_w is the rotational drag coefficient, and $\vec{\xi}$ is a Gaussian white noise. The torque is a major ingredient in the simulations, since it may reorient the alga away from the interface. We also explicitly account for the alga's run-and-tumble swimming behavior [35].

Note that all geometric and dynamic parameters that entered the simulations were either measured directly from our experiments or extracted from the literature, including a microscopic interaction time (τ_w/k_BT) at the interface [29]. We take the center of the segment connecting the centers of the small and large spheres as the dumbbell's axis of rotation. Hydrodynamic interactions are absent in this model and the dynamics are determined by steric interactions at the confining wall, where only the normal component of $\vec{F}_w$ is considered. The radial probability densities $P(r)$ were extracted from both simulations and also an analytical approach; we refer the reader to the Supplemental Material for the details of the analytics (Sec. S3, Ref. [31]). An exemplar simulation curve is presented in the inset of Fig. 3(a), and we find excellent quantitative agreement of these data with the experiments.

In order to quantify the near-wall swimming statistics, we define the near-wall swimming probability, $\Phi(r_c)$, as the relative probability of finding the alga or dumbbell towards the wall as compared to the center. In our notation, this is written as:

$$\Phi(r_c) = 1 - \frac{r_c}{r_c - b}\int_0^{r_c-b} P(r)dr, \tag{4}$$

where b is the extent of wall influence, measured from high-resolution optical micrographs of wall interaction events (see [29]) as approximately 15 μm. This corresponds to approximately the length of the flagella plus one cell radius (independent of compartment size). Figure 3(b) presents $\Phi(r_c)$ for experiments and Brownian dynamics simulations, which all agree quantitatively and show a monotonic decrease for increasing compartment radius r_c.

Analysis of the temporal swimming statistics (Sec. S4, Ref. [31]) reveals that the alga spends up to several seconds within the near-wall swimming zone for the smaller compartments. For large compartments, this time becomes comparable to the characteristic wall interaction time of about 0.15 s for a single wall interaction event [29]. Note that the alga swims with a typical velocity of 100 ± 10 μm/s, in agreement with swimming velocities reported in bulk [35]. The angular swimming statistics are based on the local swimming angle, measured relative to

the local wall tangent. Within the near-wall swimming zone, this angle features a maximum around zero degrees, indicating that the wall induces a preferred swimming direction parallel to the concave interface. Note that these angular statistics represent all navigational movement of the alga near the wall, which may include any microscopic interactions the alga might have with the boundaries.

Upon interaction with an interface, the alga reorients due to its characteristic torque with the wall and scatters off at some shallow angle (see also [29]). If the compartment is sufficiently curved, the alga will encounter another section of the interface in a short time, interact, scatter off, and continue swimming. This process will repeat itself such that, for small compartments (high curvature), it appears that the alga swims nonstop parallel to the interface in a clockwise or counterclockwise direction, since the alga will encounter another interface during its characteristic persistent swimming time. In contrast, for large compartments (low curvature), the alga will travel farther before meeting another interface. Thus, it is more likely that the alga's reorientation will direct it towards the compartment center. Nonetheless, due to the confinement the alga will encounter an interface before undergoing a run-and-tumble-like motion. The simulations and analytics capture this process: using an asymmetric dumbbell model, the alga will naturally experience a torque at the interface and reorient with a finite interaction time, subsequently encountering another interface before it can "tumble." This description is confirmed by a simultaneous comparison of concave and convex interfaces by adding a central pillar to the circular chambers. The analysis of experimental and simulated trajectories show that the alga scatters off at the pillar and escapes the convex wall (Sec. S5, Ref. [31]), consistent with studies on single microscopic scattering events [29,30].

To uncouple the effects of curvature from size-dependent geometric factors, we consider elliptical chambers. Experiments [Fig. 4(a)] and Brownian dynamics simulations [Fig. 4(b)] show a higher likelihood of finding the alga swimming in one of the apex regions of the compartments. We find in both experiments and simulations that the near-wall swimming probability density in elliptical chambers increases monotonically with the corresponding wall curvature, in line with the results obtained for circular compartments [Fig. 3(b)]. Hence, we have established unambiguous evidence that the (local) wall curvature controls the near-wall swimming effect in confinement. Note that the curvature scaling found in [38] is a consequence of assuming sliding motion along the confining surface, whereas our results derive from the dynamic action of the cell's characteristic torque at the wall due to steric wall interactions of its flagella. In contrast to the active dumbbell model, we find that a torque-free, spherical active Brownian particle cannot reproduce the experimental data. In fact, a simple active Brownian particle (e.g. [39]) strongly overestimates the magnitude of wall influence, nor does it capture the scaling with the wall curvature (Sec. S2, Ref. [31]).

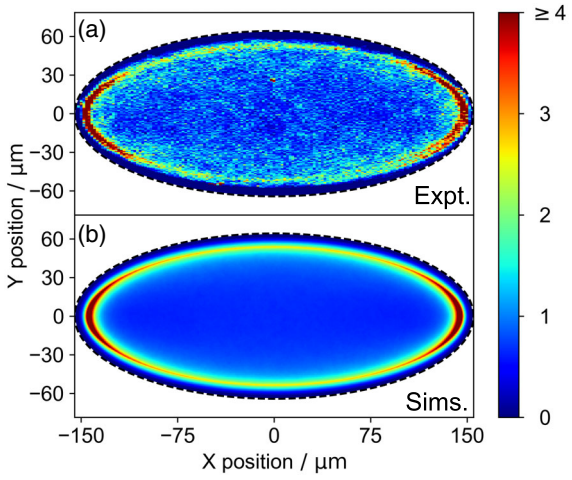

FIG. 4. Relative probability density for elliptical compartments (eccentricity = 0.91): (a) experiments and (b) simulations.

In the absence of external flow, cell-cell interactions, photo- and chemotaxes, we isolated a curvature-guided motility mechanism for a single microalga in a confined microfluidic habitat with controlled geometric properties. The concave nature of the confining walls leads to an enhanced probability of near-wall swimming for puller-type microswimmers, as quantified by a statistical analysis of experimental cell trajectories. Brownian dynamics simulations based on an active asymmetric dumbbell model quantitatively capture the experiments and validate a characteristic curvature scaling of the near-wall swimming probability. The main ingredients of this curvature guidance are the torque that the alga experiences during an interaction event with the wall, the compartment's wall curvature, and the suppression of the alga's diffusive swimming regime in confinement. Hydrodynamics are not explicitly necessary to understand this swimming behavior, yet they might be required to capture the microscopic details of flagellar interactions with interfaces [29,30]. These findings provide evidence that enhanced near-wall swimming in confinement is not exclusive to microorganisms propelling themselves by rear-mounted appendages. The fact that we track the motility of a single cell allows for dissecting the fundamental physics of a puller-type microswimmer in confinement, whereas earlier studies focused on the collective behavior of bacterial suspensions in confinement, which is governed by cell-cell interactions and excluded volume effects [40–42].

These results may pave the way towards a fundamental understanding of the motility of microorganisms in their natural habitats. A consequence of enhanced detention times at a highly curved wall is a greater likelihood for the surface-association of planktonic cells at walls, which can trigger the formation of biofilms in liquid-immersed porous media. Thus, we expect that these insights are highly relevant in environmental applications, water filtration

systems, and photobioreactors [43]. We also anticipate that these insights may inspire new design principles for the guidance of cellular motion [44–47], complementary to existing rectification approaches [29].

The authors acknowledge M. Lorenz and the Algae Culture Collection (SAG) in Göttingen, Germany. We also thank S. Herminghaus for discussions, and A. Schella and D. Lavrentovich for technical assistance. F. J. S. and M. G. M. acknowledge financial support from the DFG Collaborative Research Center SFB 937 (Project A20). O. B. acknowledges support from the Joliot ESPCI Paris Chair and the Total-ESPCI Paris Chair.

T. O. and F. J. S. contributed equally to this work.

*To whom correspondence should be addressed.
oliver.baeumchen@ds.mpg.de

[1] X. Sun, M. K. Driscoll, C. Guven, S. Das, C. A. Parent, J. T. Fourkas, and W. Losert, Proc. Natl. Acad. Sci. U.S.A. **112**, 12557 (2015).
[2] H. Wu, M. Thiébaud, W.-F. Hu, A. Farutin, S. Rafaï, M. C. Lai, P. Peyla, and C. Misbah, Phys. Rev. E **92**, 050701 (2015).
[3] H. Jeon, S. Koo, W. M. Reese, P. Loskill, C. P. Grigoropoulos, and K. E. Healy, Nat. Mater. **14**, 918 (2015).
[4] H. G. Yevick, G. Duclos, I. Bonnet, and P. Silberzan, Proc. Natl. Acad. Sci. U.S.A. **112**, 5944 (2015).
[5] M. Delarue, J. Hartung, C. Schreck, P. Gniewek, L. Hu, S. Herminghaus, and O. Hallatschek, Nat. Phys. **12**, 762 (2016).
[6] H. C. Berg and L. Turner, Biophys. J. **58**, 919 (1990).
[7] W. Yan and J. F. Brady, J. Fluid Mech. **785**, R1 (2015).
[8] R. U. Meckenstock *et al.*, Science **345**, 673 (2014).
[9] J. Wierzchos, A. de los Ríos, and C. Ascaso, Int. Microbiol. **15**, 171 (2012).
[10] C. K. Robinson *et al.*, Environ. Microbiol. **17**, 299 (2015).
[11] L. Ranjard and A. Richaume, Res. Microbiol. **152**, 707 (2001).
[12] M. Eisenbach and L. C. Giojalas, Nat. Rev. Mol. Cell Biol. **7**, 276 (2006).
[13] P. Denissenko, V. Kantsler, D. J. Smith, and J. Kirkman-Brown, Proc. Natl. Acad. Sci. U.S.A. **109**, 8007 (2012).
[14] V. Kantsler, J. Dunkel, M. Blayney, and R. E. Goldstein, eLife **3**, e02403 (2014).
[15] R. Nosrati, A. Driouchi, C. M. Yip, and D. Sinton, Nat. Commun. **6**, 8703 (2015).
[16] N. Heddergott, T. Krüger, S. B. Babu, A. Wei, E. Stellamanns, S. Uppaluri, T. Pfohl, H. Stark, M. Engstler, and S. M. Beverley, PLoS Pathogens **8**, e1003023 (2012).
[17] P. Watnick and R. Kolter, J. Bacteriol. **182**, 2675 (2000).
[18] L. Hall-Stoodley, J. W. Costerton, and P. Stoodley, Nat. Rev. Microbiol. **2**, 95 (2004).
[19] H.-C. Flemming and J. Wingender, Nat. Rev. Microbiol. **8**, 623 (2010).
[20] M. G. Mazza, J. Phys. D **49**, 203001 (2016).
[21] E. Lauga and T. R. Powers, Rep. Prog. Phys. **72**, 096601 (2009).
[22] T. Brotto, J.-B. Caussin, E. Lauga, and D. Bartolo, Phys. Rev. Lett. **110**, 038101 (2013).
[23] J. Elgeti, R. G. Winkler, and G. Gompper, Rep. Prog. Phys. **78**, 056601 (2015).
[24] K. Drescher, J. Dunkel, L. H. Cisneros, S. Ganguly, and R. E. Goldstein, Proc. Natl. Acad. Sci. U.S.A. **108**, 10940 (2011).
[25] K. Drescher, R. E. Goldstein, N. Michel, M. Polin, and I. Tuval, Phys. Rev. Lett. **105**, 168101 (2010).
[26] J. S. Guasto, K. A. Johnson, and J. P. Gollub, Phys. Rev. Lett. **105**, 168102 (2010).
[27] K. C. Leptos, J. S. Guasto, J. P. Gollub, A. I. Pesci, and R. E. Goldstein, Phys. Rev. Lett. **103**, 198103 (2009).
[28] E. Lushi, V. Kantsler, and R. E. Goldstein, Phys. Rev. E **96**, 023102 (2017).
[29] V. Kantsler, J. Dunkel, M. Polin, and R. E. Goldstein, Proc. Natl. Acad. Sci. U.S.A. **110**, 1187 (2013).
[30] M. Contino, E. Lushi, I. Tuval, V. Kantsler, and M. Polin, Phys. Rev. Lett. **115**, 258102 (2015).
[31] See Supplemental Material at http://link.aps.org/supplemental/10.1103/PhysRevLett.120.068002 for further details on the experimental methods and Brownian dynamics simulations, including the temporal and angular statistics of near-wall swimming and motility in compartments exhibiting concave and convex interfaces. The Supplemental Material also contains the derivation and details of an analytical model, a movie of a typical experiment, as well as Refs. [32–34].
[32] J. C. Crocker and D. G. Grier, J. Colloid Interface Sci. **179**, 298 (1996).
[33] S. E. Spagnolie, G. R. Moreno-Flores, D. Bartolo, and E. Lauga, Soft Matter **11**, 3396 (2015).
[34] D. Takagi, J. Palacci, A. B. Braunschweig, M. J. Shelley, and J. Zhang, Soft Matter **10**, 1784 (2014).
[35] M. Polin, I. Tuval, K. Drescher, J. P. Gollub, and R. E. Goldstein, Science **325**, 487 (2009).
[36] A. Wysocki, J. Elgeti, and G. Gompper, Phys. Rev. E **91**, 050302(R) (2015).
[37] J. D. Weeks, D. Chandler, and H. C. Andersen, J. Chem. Phys. **54**, 5237 (1971).
[38] Y. Fily, A. Baskaran, and M. F. Hagan, Soft Matter **10**, 5609 (2014).
[39] S. E. Spagnolie, C. Wahl, J. Lukasik, and J.-L. Thiffeault, Physica (Amsterdam) **341D**, 33 (2017).
[40] H. Wioland, F. G. Woodhouse, J. Dunkel, J. O. Kessler, and R. E. Goldstein, Phys. Rev. Lett. **110**, 268102 (2013).
[41] I. D. Vladescu, E. J. Marsden, J. Schwarz-Linek, V. A. Martinez, J. Arlt, A. N. Morozov, D. Marenduzzo, M. E. Cates, and W. C. K. Poon, Phys. Rev. Lett. **113**, 268101 (2014).
[42] E. Lushi, H. Wioland, and R. E. Goldstein, Proc. Natl. Acad. Sci. U.S.A. **111**, 9733 (2014).
[43] P. M. Schenk, S. R. Thomas-Hall, E. Stephens, U. C. Marx, J. H. Mussgnug, C. Posten, O. Kruse, and B. Hankamer, Bioenergy Res. **1**, 20 (2008).

[44] D. B. Weibel, P. Garstecki, D. Ryan, W. R. DiLuzio, M. Mayer, J. E. Seto, and G. M. Whitesides, Proc. Natl. Acad. Sci. U.S.A. **102**, 11963 (2005).

[45] X. Ai, Q. Liang, M. Luo, K. Zhang, J. Pan, and G. Luo, Lab Chip **12**, 4516 (2012).

[46] S. K. Min, G. H. Yoon, J. H. Joo, S. J. Sim, and H. S. Shin, Sci. Rep. **4**, 4675 (2014).

[47] S. Das, A. Garg, A. I. Campbell, J. Howse, A. Sen, D. Velegol, R. Golestanian, and S. J. Ebbens, Nat. Commun. **6**, 8999 (2015).